14th European Signal Processing Conference (EUSIPCO 2006), Florence, Italy, September 4-8, 2006, copyright by EURASIP

STATISTICAL PROPERTIES OF THE FXLMS-BASED NARROWBAND ACTIVE NOISE CONTROL SYSTEM

Yegui Xiao[†], *Kouji Hasegawa*[†], *Akira Ikuta*[†], *Kentaro Noguchi*[††]

[†] Dept. of Management & Information Systems, Prefectural University of Hiroshima
1-1-71 Ujina-Higashi, Minami-ku, Hiroshima, Japan 734-8558
xiao@pu-hiroshima.ac.jp
[††] Okinawa National College of Technology, Okinawa, Japan 905-2192

ABSTRACT

Noise signals generated by rotating machines such as diesel engines, cutting machines, fans, etc. may be modeled as noisy sinusoidal signals which can be successfully suppressed by narrowband active noise control (ANC) systems. In this paper, the statistical performance of such a conventional filtered-X LMS (FXLMS) based narrowband ANC system is investigated in detail. First, difference equations governing the dynamics of the system are derived in terms of convergence of the mean and mean square estimation errors for the discrete Fourier coefficients (DFC) of the secondary source. Steady-state expressions for DFC estimation mean square error (MSE) as well as the remaining noise power are then developed in closed forms. A stability bound for the FXLMS in the mean sense is also derived. Extensive simulations are performed to demonstrate the validity of the analytical findings.

1. INTRODUCTION

There are many rotating machines such as diesel engines, cutting machines, fans, etc. which produce noise signals that are harmful to working and living environment. Usually, these noise signals may be modeled as sinusoidal signals in additive noise. Removing or reducing these noise signals, especially their lower frequency portion, is very important in various engineering and environmental systems. Narrowband active noise control (ANC) systems are designated to reduce or mitigate these annoying noise signals [1]-[7].

A vast number of ANC systems have been proposed. Usually, the finite-impulse-response (FIR) filters adapted by a filtered-X least mean square (FXLMS) algorithm and its variants are applied [3]. Other techniques using recursive least squares (RLS) and Kalman filtering based algorithms have also been developed for many ANC systems [6, 3], which generally provide better noise reduction performance at the expense of more computational cost.

The conventional narrowband ANC systems are effective in suppressing sinusoidal noise in many real-life applications [3]. Fig.1 shows such a conventional ANC system [3, 4]. Some preliminary analysis of the system in the frequency domain is given in [3, 4], but statistical properties of the system has not been investigated yet.

In this paper, performance analysis of this FXLMS-based ANC system is performed in detail. Difference equations governing the dynamics of the system are developed in terms of estimation error between the DFCs estimates of the secondary source and their optimal values which assure perfect cancellation for all the primary sinusoids being targeted. The steady-state DFC estimation mean square error (MSE) as well as the remaining noise power are also derived in closed forms. A stability bound in the mean sense is also derived. Extensive simulations are conducted to prove the validity of the analytical results.

The primary noise signal in Fig. 1 to be removed is given by

$$p(n) = \sum_{i=1}^{q}\{a_i\cos(\omega_i n)+b_i\sin(\omega_i n)\}+v_p(n) \quad (1)$$

where q is the number of frequency components of the sinusoidal signal, ω_i is the frequency of the i-th component, $v_p(n)$ is a zero-mean additive white Gaussian noise with variance σ_p^2. The signal frequencies may be identified in a regression fashion based on a synchronization (sync) signal derived from a non-acoustical sensor like a tachometer.

The secondary source is expressed by

$$y(n) = \sum_{i=1}^{q} y_i(n)=\sum_{i=1}^{q}\left\{\hat{a}_i(n)x_{a_i}(n)+\hat{b}_i(n)x_{b_i}(n)\right\} \quad (2)$$

$$x_{a_i}(n) = \cos(\omega_i n), \quad x_{b_i}(n)=\sin(\omega_i n) \quad (3)$$

The FXLMS algorithm for DFC estimates is given by

$$\hat{a}_i(n+1) = \hat{a}_i(n)+\mu_i e(n)\hat{x}_{a_i}(n) \quad (4)$$

$$\hat{b}_i(n+1) = \hat{b}_i(n)+\mu_i e(n)\hat{x}_{b_i}(n) \quad (5)$$

where

$$e(n) = p(n)-y_p(n), \; y_p(n)=S(z)y(n) \quad (6)$$

$$\hat{x}_{a_i}(n) = \hat{S}(z)x_{a_i}(n)=\hat{\alpha}_i x_{a_i}(n)+\hat{\beta}_i x_{b_i}(n) \quad (7)$$

$$\hat{x}_{b_i}(n) = \hat{S}(z)x_{b_i}(n)=-\hat{\beta}_i x_{a_i}(n)+\hat{\alpha}_i x_{b_i}(n) \quad (8)$$

$$S(z) = \sum_{j=0}^{M-1} s_j z^{-j}, \; \hat{S}(z)=\sum_{j=0}^{\hat{M}-1}\hat{s}_j z^{-j} \quad (9)$$

$$\hat{\alpha}_i = \sum_{j=0}^{\hat{M}-1}\hat{s}_j\cos(j\omega_i), \quad \hat{\beta}_i=\sum_{j=0}^{\hat{M}-1}\hat{s}_j\sin(j\omega_i) \quad (10)$$

$S(z)$ is the true secondary path, $\hat{S}(z)$ is an estimate of $S(z)$, which is obtained in advance by some parameter identification technique and is usually assumed to be close to $S(z)$, M and $\hat{M}$ are the system orders of the true and estimated secondary paths, respectively.

2. PERFORMANCE ANALYSIS

The error signal (residual noise) $e(n)$ is given by

$$\begin{aligned} e(n) &= p(n) - S(z)y(n) \qquad (11) \\ &\approx \sum_{i=1}^{q} \Big\{ [a_i - (\alpha_i \hat{a}_i(n) - \beta_i \hat{b}_i(n))] x_{a_i}(n) \\ &\qquad [b_i - (\beta_i \hat{a}_i(n) + \alpha_i \hat{b}_i(n))] x_{b_i}(n) \Big\} + v_p(n) \end{aligned}$$

where

$$\begin{aligned} \hat{a}_i(n-j) &\approx \hat{a}_i(n),\ j = 1, 2, \cdots, M-1 \\ \hat{b}_i(n-j) &\approx \hat{b}_i(n),\ j = 1, 2, \cdots, M-1 \end{aligned}$$

are used to facilitate and simplify the analysis that follows. Fortunately, extensive simulations reveal that this does not affect the accuracy of analysis significantly even for relatively fast adaptation (see simulation results in Section 3). Obviously, from (11), optimal DFCs for a perfect cancellation of all the sinusoids are given by

$$\begin{bmatrix} a_{i,opt} \\ b_{i,opt} \end{bmatrix} = \begin{bmatrix} \alpha_i & -\beta_i \\ \beta_i & \alpha_i \end{bmatrix}^{-1} \begin{bmatrix} a_i \\ b_i \end{bmatrix} \qquad (12)$$

where

$$\alpha_i = \sum_{j=0}^{M-1} s_j \cos(j\omega_i), \quad \beta_i = \sum_{j=0}^{M-1} s_j \sin(j\omega_i) \qquad (13)$$

Define the estimation errors of DFCs as

$$\varepsilon_{a_i}(n) = a_{i,opt} - \hat{a}_i(n), \quad \varepsilon_{b_i}(n) = b_{i,opt} - \hat{b}_i(n) \qquad (14)$$

The error signal reduces to

$$\begin{aligned} e(n) \approx & \sum_{i=1}^{q} \{ [\alpha_i \varepsilon_{a_i}(n) - \beta_i \varepsilon_{b_i}(n)] x_{a_i}(n) \\ & [\beta_i \varepsilon_{a_i}(n) + \alpha_i \varepsilon_{b_i}(n)] x_{b_i}(n) \} + v_p(n) \qquad (15) \end{aligned}$$

A. Convergence in the mean sense

Putting the above error signal and (14) in the FXLMS recursions and taking ensemble average, one yields

$$\begin{aligned} E[\varepsilon_{a_k}(n+1)] &= \left\{ 1 - \frac{1}{2}\mu_k(\alpha_k \hat{\alpha}_k + \beta_k \hat{\beta}_k) \right\} E[\varepsilon_{a_k}(n)] \qquad (16) \\ &\quad - \frac{1}{2}\mu_k(-\hat{\alpha}_k \beta_k + \alpha_k \hat{\beta}_k) E[\varepsilon_{b_k}(n)] \\ E[\varepsilon_{b_k}(n+1)] &= \left\{ 1 - \frac{1}{2}\mu_k(\alpha_k \hat{\alpha}_k + \beta_k \hat{\beta}_k) \right\} E[\varepsilon_{b_k}(n)] \qquad (17) \\ &\quad - \frac{1}{2}\mu_k(-\alpha_k \hat{\beta}_k + \hat{\alpha}_k \beta_k) E[\varepsilon_{a_k}(k)] \end{aligned}$$

In the above derivations, $x_{a_i}(n)$ and $x_{b_i}(n)$ are treated as pseudo-random noise [1, 7].

B. Convergence in the mean square sense

Using (14) and (15) in (4) and squaring both sides of it, one gets

$$\begin{aligned} E[\varepsilon^2_{a_k}(n+1)] = & E[\varepsilon^2_{a_k}(n)] \qquad (18) \\ & -2\mu_k \underbrace{E[\varepsilon_{a_k}(n) e(n) \hat{x}_{a_k}(n)]}_{I_k(n)} \\ & +\mu_k^2 \underbrace{E[e^2(n) \hat{x}^2_{a_k}(n)]}_{J_k(n)} \end{aligned}$$

After very lengthy and complicated calculations, one may reach

$$\begin{aligned} I_k(n) = & \frac{1}{2}(\alpha_k \hat{\alpha}_k + \beta_k \hat{\beta}_k) E[\varepsilon^2_{a_k}(n)] \qquad (19) \\ & + \frac{1}{2}(\alpha_k \hat{\beta}_k - \hat{\alpha}_k \beta_k) E[\varepsilon_{a_k}(n)] E[\varepsilon_{b_k}(n)] \end{aligned}$$

$$\begin{aligned} J_k(n) = & \frac{1}{2}\sigma_p^2(\hat{\alpha}_k^2 + \hat{\beta}_k^2) \qquad (20) \\ & + \frac{3}{8}\hat{\alpha}_k^2 \{ \alpha_k^2 E[\varepsilon^2_{a_k}(n)] + \beta_k^2 E[\varepsilon^2_{b_k}(n)] \\ & \qquad -2\alpha_k \beta_k E[\varepsilon_{a_k}(n)] E[\varepsilon_{b_k}(n)] \} \\ & + \frac{1}{4}\hat{\alpha}_k^2 \sum_{i=1, i\neq k}^{q} \{ \alpha_i^2 E[\varepsilon^2_{a_i}(n)] + \beta_i^2 E[\varepsilon^2_{b_i}(n)] \\ & \qquad -2\alpha_i \beta_i E[\varepsilon_{a_i}(n)] E[\varepsilon_{b_i}(n)] \} \\ & + \frac{1}{8}\hat{\alpha}_k^2 \{ \beta_k^2 E[\varepsilon^2_{a_k}(n)] + \alpha_k^2 E[\varepsilon^2_{b_k}(n)] \\ & \qquad +2\alpha_k \beta_k E[\varepsilon_{a_k}(n)] E[\varepsilon_{b_k}(n)] \} \\ & + \frac{1}{4}\hat{\alpha}_k^2 \sum_{i=1, i\neq k}^{q} \{ \beta_i^2 E[\varepsilon^2_{a_i}(n)] + \alpha_i^2 E[\varepsilon^2_{b_i}(n)] \\ & \qquad +2\alpha_i \beta_i E[\varepsilon_{a_i}(n)] E[\varepsilon_{b_i}(n)] \} \\ & + \frac{1}{2}\hat{\alpha}_k \hat{\beta}_k \{ \alpha_k \beta_k (E[\varepsilon^2_{a_k}(n)] - E[\varepsilon^2_{b_k}(n)]) \\ & \qquad +(\alpha_k^2 - \beta_k^2) E[\varepsilon_{a_k}(n)] E[\varepsilon_{b_k}(n)] \} \\ & + \frac{1}{8}\hat{\beta}_k^2 \{ \alpha_k^2 E[\varepsilon^2_{a_k}(n)] + \beta_k^2 E[\varepsilon^2_{b_k}(n)] \\ & \qquad -2\alpha_k \beta_k E[\varepsilon_{a_k}(n)] E[\varepsilon_{b_k}(n)] \} \\ & + \frac{1}{4}\hat{\beta}_k^2 \sum_{i=1, i\neq k}^{q} \{ \alpha_i^2 E[\varepsilon^2_{a_i}(n)] + \beta_i^2 E[\varepsilon^2_{b_i}(n)] \\ & \qquad -2\alpha_i \beta_i E[\varepsilon_{a_i}(n)] E[\varepsilon_{b_i}(n)] \} \\ & + \frac{3}{8}\hat{\beta}_k^2 \{ \beta_k^2 E[\varepsilon^2_{a_k}(n)] + \alpha_k^2 E[\varepsilon^2_{b_k}(n)] \\ & \qquad +2\alpha_k \beta_k E[\varepsilon_{a_k}(n)] E[\varepsilon_{b_k}(n)] \} \\ & + \frac{1}{4}\hat{\beta}_k^2 \sum_{i=1, i\neq k}^{q} \{ \beta_i^2 E[\varepsilon^2_{a_i}(n)] + \alpha_i^2 E[\varepsilon^2_{b_i}(n)] \\ & \qquad +2\alpha_i \beta_i E[\varepsilon_{a_i}(n)] E[\varepsilon_{b_i}(n)] \} \end{aligned}$$

Similarly, one has from (5)

$$\begin{aligned} E[\varepsilon^2_{b_k}(n+1)] = & E[\varepsilon^2_{b_k}(n)] \qquad (21) \\ & -2\mu_k \underbrace{E[\varepsilon_{b_k}(n) e(n) \hat{x}_{b_k}(n)]}_{K_k(n)} \\ & +\mu_k^2 \underbrace{E[e^2(n) \hat{x}^2_{b_k}(n)]}_{N_k(n)} \end{aligned}$$

where $K_k(n)$ and $N_k(n)$ can be derived in the same way that $I_k(n)$ and $J_k(n)$ are calculated.

$$\begin{aligned} K_k(n) &= \frac{1}{2}(\alpha_k\hat{\alpha}_k+\beta_k\hat{\beta}_k)E[\varepsilon^2_{b_k}(n)] \\ &\quad+\frac{1}{2}(-\alpha_k\hat{\beta}_k+\hat{\alpha}_k\beta_k)E[\varepsilon_{a_k}(n)]E[\varepsilon_{b_k}(n)] \end{aligned} \tag{22}$$

$$\begin{aligned} N_k(n) &= \frac{1}{2}\sigma_p^2(\hat{\alpha}_k^2+\hat{\beta}_k^2) \\ &+\frac{3}{8}\hat{\beta}_k^2\{\alpha_k^2E[\varepsilon^2_{a_k}(n)]+\beta_k^2E[\varepsilon^2_{b_k}(n)] \\ &\qquad -2\alpha_k\beta_kE[\varepsilon_{a_k}(n)]E[\varepsilon_{b_k}(n)]\} \\ &+\frac{1}{4}\hat{\beta}_k^2\sum_{i=1,i\neq k}^{q}\{\alpha_i^2E[\varepsilon^2_{a_i}(n)]+\beta_i^2E[\varepsilon^2_{b_i}(n)] \\ &\qquad -2\alpha_i\beta_iE[\varepsilon_{a_i}(n)]E[\varepsilon_{b_i}(n)]\} \\ &+\frac{1}{8}\hat{\beta}_k^2\{\beta_k^2E[\varepsilon^2_{a_k}(n)]+\alpha_k^2E[\varepsilon^2_{b_k}(n)] \\ &\qquad +2\alpha_k\beta_kE[\varepsilon_{a_k}(n)]E[\varepsilon_{b_k}(n)]\} \\ &+\frac{1}{4}\hat{\beta}_k^2\sum_{i=1,i\neq k}^{q}\{\beta_i^2E[\varepsilon^2_{a_i}(n)]+\alpha_i^2E[\varepsilon^2_{b_i}(n)] \\ &\qquad +2\alpha_i\beta_iE[\varepsilon_{a_i}(n)]E[\varepsilon_{b_i}(n)]\} \\ &-\frac{1}{2}\hat{\alpha}_k\hat{\beta}_k\{\alpha_k\beta_k(E[\varepsilon^2_{a_k}(n)]-E[\varepsilon^2_{b_k}(n)]) \\ &\qquad +(\alpha_k^2-\beta_k^2)E[\varepsilon_{a_k}(n)]E[\varepsilon_{b_k}(n)]\} \\ &+\frac{1}{8}\hat{\alpha}_k^2\{\alpha_k^2E[\varepsilon^2_{a_k}(n)]+\beta_k^2E[\varepsilon^2_{b_k}(n)] \\ &\qquad -2\alpha_k\beta_kE[\varepsilon_{a_k}(n)]E[\varepsilon_{b_k}(n)]\} \\ &+\frac{1}{4}\hat{\alpha}_k^2\sum_{i=1,i\neq k}^{q}\{\alpha_i^2E[\varepsilon^2_{a_i}(n)]+\beta_i^2E[\varepsilon^2_{b_i}(n)] \\ &\qquad -2\alpha_i\beta_iE[\varepsilon_{a_i}(n)]E[\varepsilon_{b_i}(n)]\} \\ &+\frac{3}{8}\hat{\alpha}_k^2\{\beta_k^2E[\varepsilon^2_{a_k}(n)]+\alpha_k^2E[\varepsilon^2_{b_k}(n)] \\ &\qquad +2\alpha_k\beta_kE[\varepsilon_{a_k}(n)]E[\varepsilon_{b_k}(n)]\} \\ &+\frac{1}{4}\hat{\alpha}_k^2\sum_{i=1,i\neq k}^{q}\{\beta_i^2E[\varepsilon^2_{a_i}(n)]+\alpha_i^2E[\varepsilon^2_{b_i}(n)] \\ &\qquad +2\alpha_i\beta_iE[\varepsilon_{a_i}(n)]E[\varepsilon_{b_i}(n)]\} \end{aligned} \tag{23}$$

C. Steady-state MSE expressions

When the FXLMS algorithm reaches its steady state ($n\to\infty$), it is easy to see, from the derived difference equations for the mean error, that

$$E[\varepsilon_{a_i}(n)]|_{n\to\infty}=E[\varepsilon_{a_i}(\infty)]=0 \tag{24}$$
$$E[\varepsilon_{b_i}(n)]|_{n\to\infty}=E[\varepsilon_{b_i}(\infty)]=0 \tag{25}$$

which implies that the DFC estimates converges to their optimal values as long as the system is statistically stable. Using these in the difference equations for the MSE ((18) and (21)) and subtracting (21) from (18), one has

$$\begin{aligned} &(\alpha_k\hat{\alpha}_k+\beta\hat{\beta}_k)\left(E[\varepsilon^2_{a_k}(\infty)]-E[\varepsilon^2_{b_k}(\infty)]\right) \\ &=\frac{1}{4}\mu_k\left\{(\alpha_k^2-\beta_k^2)(\hat{\alpha}_k^2-\hat{\beta}_k^2)+4\alpha_k\beta_k\hat{\alpha}_k\hat{\beta}_k\right\} \\ &\qquad\times\left(E[\varepsilon^2_{a_k}(\infty)]-E[\varepsilon^2_{b_k}(\infty)]\right) \end{aligned} \tag{26}$$

Obviously,

$$E[\varepsilon^2_{a_k}(\infty)]=E[\varepsilon^2_{b_k}(\infty)] \tag{27}$$

holds. Substituting (24), (25) and (27) in (18) leads to

$$\begin{aligned} &(\alpha_k\hat{\alpha}_k+\beta\hat{\beta}_k)E[\varepsilon^2_{a_k}(\infty)]= \\ &\frac{1}{2}\mu_k\sigma_p^2(\hat{\alpha}_k^2+\hat{\beta}_k^2)+\frac{1}{2}\mu_k(\hat{\alpha}_k^2+\hat{\beta}_k^2)\sum_{i=1}^{q}(\alpha_i^2+\beta_i^2)E[\varepsilon^2_{a_i}(\infty)] \end{aligned} \tag{28}$$

Multiplying both sides of the above equation with $(\alpha_k^2+\beta_k^2)/(\alpha_k\hat{\alpha}_k+\beta_k\hat{\beta}_k)$ and then taking summation with respect to k, one obtains

$$\sum_{i=1}^{q}(\alpha_i^2+\beta_i^2)E[\varepsilon^2_{a_i}(\infty)]=\frac{\eta\sigma_p^2}{1-\eta} \tag{29}$$

where
$$\eta=\frac{1}{2}\sum_{m=1}^{q}\mu_m\frac{(\alpha_m^2+\beta_m^2)(\hat{\alpha}_m^2+\hat{\beta}_m^2)}{\alpha_m\hat{\alpha}_m+\beta_m\hat{\beta}_m} \tag{30}$$

Putting (29) back to (28) readily gives

$$E[\varepsilon^2_{a_k}(\infty)]=\frac{1}{2}\mu_k\frac{\hat{\alpha}_k^2+\hat{\beta}_k^2}{\alpha_k\hat{\alpha}_k+\beta_k\hat{\beta}_k}\frac{\sigma_p^2}{1-\eta} \tag{31}$$

The remaining noise power at steady state is ultimately derived as

$$E[e^2(\infty)]\;=\;\sigma_p^2+\sum_{i=1}^{q}(\alpha_i^2+\beta_i^2)E[\varepsilon^2_{a_i}(\infty)]=\frac{\sigma_p^2}{1-\eta} \tag{32}$$

D. A stability bound in the mean sense

From the linear difference equations, (16) and (17), for the convergence in the mean, we have

$$\begin{aligned} &|\mathbf{G}_k-\lambda\mathbf{I}_2| \;= \\ &\begin{vmatrix} 1-\frac{1}{2}\mu_k(\alpha_k\hat{\alpha}_k+\beta_k\hat{\beta}_k)-\lambda & -\frac{1}{2}\mu_k(-\hat{\alpha}_k\beta_k+\alpha_k\hat{\beta}_k) \\ \frac{1}{2}\mu_k(-\alpha_k\hat{\beta}_k+\hat{\alpha}_k\beta_k) & 1-\frac{1}{2}\mu_k(\alpha_k\hat{\alpha}_k+\beta_k\hat{\beta}_k)-\lambda \end{vmatrix}=0 \end{aligned} \tag{33}$$

where $\mathbf{G}_k$ is the coefficient matrix, and $\mathbf{I}_2$ is a unit matrix of 2×2. λ is the eigenvalue of $\mathbf{G}_k$. Let $\lambda=\lambda_r+\sqrt{-1}\lambda_c$. Putting the complex part of (33) to zero, one faces two cases. First, if $\lambda_c=0$, then

$$\begin{aligned} &\{\lambda_r-(1-\frac{1}{2}\mu_k(\alpha_k\hat{\alpha}_k+\beta_k\hat{\beta}_k)\}^2 \\ &\quad+\frac{1}{4}\mu_k^2(-\alpha_k\hat{\beta}_k+\hat{\alpha}_k\beta_k)(-\hat{\alpha}_k\beta_k+\alpha_k\hat{\beta}_k)=0 \end{aligned} \tag{34}$$

If $\lambda_r=1$, (34) produces $\mu_k=0$, which can be regarded as a lower bound for the step size. If $\lambda_r=-1$, (34) forces μ_k to be complex or negative. Second, if $\lambda_c\neq 0$, then

$$\lambda_r=1-\frac{1}{2}\mu_k(\alpha_k\hat{\alpha}_k+\beta_k\hat{\beta}_k) \tag{35}$$

Using the above equation and $\lambda_r^2+\lambda_c^2=1$ in the real part of (33) yields

$$\frac{1}{4}\Big\{(\alpha_k\hat{\alpha}_k+\beta_k\hat{\beta}_k)^2+(-\alpha_k\hat{\beta}_k+\hat{\alpha}_k\beta_k) \times(-\hat{\alpha}_k\beta_k+\alpha_k\hat{\beta}_k)\Big\}\mu_k^2-(\alpha_k\hat{\alpha}_k+\beta_k\hat{\beta}_k)\mu_k=0 \quad (36)$$

which eventually gives a upper stability bound for the step size μ_k as follows

$$\mu_{k,bound} = \frac{4(\alpha_k\hat{\alpha}_k+\beta_k\hat{\beta}_k)}{(\alpha_k\hat{\alpha}_k+\beta_k\hat{\beta}_k)^2+(-\alpha_k\hat{\beta}_k+\hat{\alpha}_k\beta_k)(-\hat{\alpha}_k\beta_k+\alpha_k\hat{\beta}_k)} \quad (37)$$

Now we have following comments in order regarding all the analytical results obtained in this Section.

C1 If the estimated secondary path $\hat{S}(z)$ is the same as its truth $S(z)$, then $\hat{\alpha}_k=\alpha_k$ and $\hat{\beta}_k=\beta_k$ and the 2nd terms in right-hand sides (RHS) of the linear difference equations (16) and (17) for the convergence in the mean sense will vanish. Therefore, the DFC mean errors become independent with each other, and a stability bound for the step size parameter can be easily derived from (16) or (17) as $\mu_{k,bound}=4/(\alpha_k^2+\beta_k^2)$, which is identical to (37).

C2 The difference equations for the convergence in the mean square sense are also of linear nature if one regards $E[\varepsilon_{a_i}(n)]E[\varepsilon_{b_i}(n)] \quad (i=1,2,\cdots,q)$ involved in (18) and (21) as time-varying driving terms. Dynamics of the algorithm in the mean square can be obtained by solving the difference equations for the convergence in the mean and mean square senses simultaneously. A tighter stability bound may be obtained based on a grid search by numerically solving these difference equations repeatedly.

C3 From (32), we see that the remaining noise power will be always larger than that of the additive white noise residing in the primary noise as long as $\hat{S}(z)$ is so close to $S(z)$ that $\hat{\alpha}_k\approx\alpha_k$ and $\hat{\beta}_k\approx\beta_k$, as η is positive in such a case. The denominator of η, $\alpha_m\hat{\alpha}_m+\beta_m\hat{\beta}_m$ may become negative by using some special $\hat{S}(z)$ such as z^{-t} (t is a properly selected integer). However, this may make the stability bound (37) become negative.

C4 In theory, users have freedom in selecting the secondary path $\hat{S}(z)$ that makes (37) and η positive. One such a case will be shown in next Section. This implies interestingly that there is no need to estimate the secondary path at all, if one can find a good guess that makes the system work. But this is not practical, and a coarse guess is basically needed.

3. SIMULATIONS

Extensive simulations are performed to demonstrate the validity of the analytical results. In all the simulations, the true secondary path $S(z)$ is generated by a Matlab lowpass filter function (FIR1) with filter order M and cutoff frequency 0.4π. The secondary path $\hat{S}(z)$ is estimated based on the system identification configuration with white noise excitation and the LMS algorithm. The ANC system is simulated after $S(z)$ is generated and its substitute $\hat{S}(z)$ is estimated. Some typical simulation results are given below.

First, the difference equations for the convergence in the mean and mean square senses are compared to the simulated dynamics of the algorithm in Fig.2, where $\hat{M}$ (20) is much smaller than its truth M (41). Apparently, the analytical results provide excellent agreement with the simulation. When $\hat{M}$ is set smaller than 20, both theory and simulation diverged. This confirms the fact that relatively shorter error path may be used in narrowband ANC systems. Second, comparisons between theory and simulations are given in Fig.3, where $\hat{M}$ (45) is larger than its truth M (41). It has been found that theory is always very close to the simulated values as long as $\hat{M}\geq M$. Third, Fig.4 shows simulations and theoretical results for a case that a pure delay is selected as the error path. Obviously, the system is stable and the theory explains simulations quite well. Fourth, the steady-state MSE expression is compared to the simulated points in Fig.5. A very good fit is observed.

4. CONCLUSIONS

In this paper, dynamics, steady-state properties and a stability bound for the convergence in the mean sense are derived for the FXLMS based ANC system. Simulations have been conducted to prove the validity of the analytical findings.

REFERENCES

[1] B. Widrow et al., *"Adaptive noise canceling: Principles and applications,"* Proc. IEEE, vol. 63, pp. 1692-1716, Dec. 1975.

[2] P. A. Nelson and S. J. Elliott, *Active Control of Sound,* Academic Press INC., 3rd ed., 1995.

[3] S. M. Kuo and D. R. Morgan, *Active Noise Control Systems, Algorithms and DSP Implementations,* John Wiley & Sons, INC., 1996.

[4] S. M. Kuo and M. J. Ji, *"Development and analysis of an adaptive noise equalizer,"* IEEE Trans. on Speech & Audio Processing, vol.3 no.3, pp.217-222, 1995.

[5] L. J. Eriksson, *"Development of the filtered-U algorithm for active noise control,"* J. Acoust. Soc. Am., 89(1), pp. 257-265, Jan. 1991.

[6] P. A. C. Lopes and M. S. Piedade, *"A Kalman filter approach to active noise control,"* in Proc. EUSIPCO 2000, Finland, 2000.

[7] Y. Xiao, L. Ma, K. Khorosani, A. Ikuta, *"A new robust narrowband active noise control system in the presence of frequency mismatch,"* IEEE Trans. on Audio, Speech & Language Processing, in press, 2006.

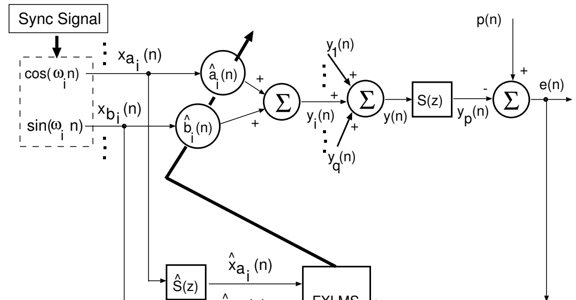

Fig. 1 The conventional narrowband ANC system (i-th channel).

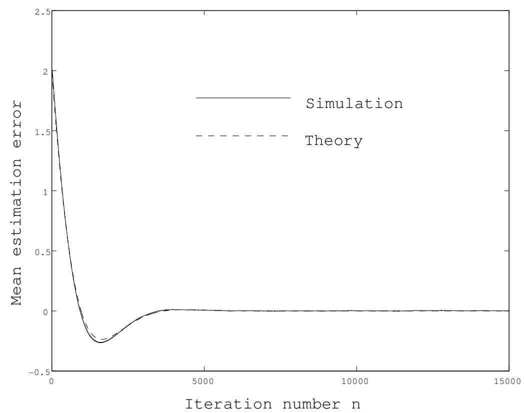

Fig.2(a) Estimation error $E[\varepsilon_{a_1}(n)]$.

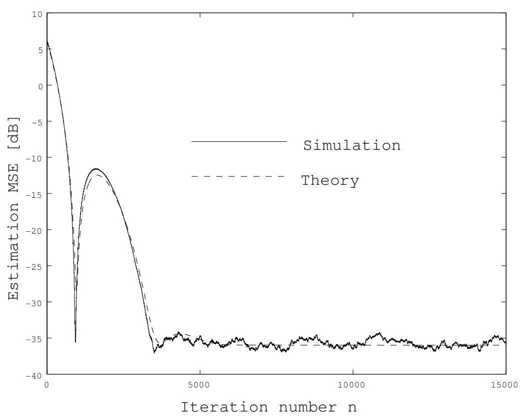

Fig.2(b) Estimation MSE $E[\varepsilon^2_{a_1}(n)]$.

Fig. 2 Comparisons between theory and simulations (signal frequency: $\omega_0 = 0.10\pi,\ 0.20\pi,\ 0.30\pi$, $a_1 = 2.0$, $b_1 = -1.0$, $a_2 = 1.0$, $b_2 = -0.5$,$a_3 = 0.5$, $b_3 = 0.1$, $\mu_1 = \mu_2 = \mu_3 = 0.01$, $\sigma_p = 0.33$, $M = 41$, $\hat{M} = 20$, 100 runs).

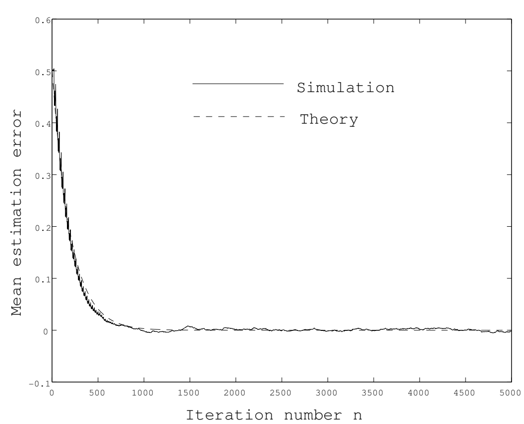

Fig.3(a) Estimation error $E[\varepsilon_{a_1}(n)]$.

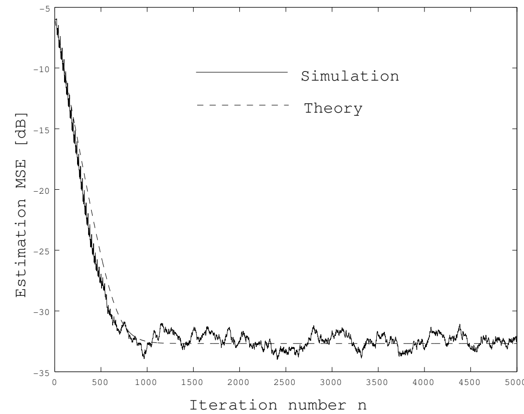

Fig.3(b) Estimation MSE $E[\varepsilon^2_{a_1}(n)]$.

Fig. 3 Comparisons between theory and simulations ($M = 41$, $\hat{M} = 45$, other conditions the same as in Fig.2).

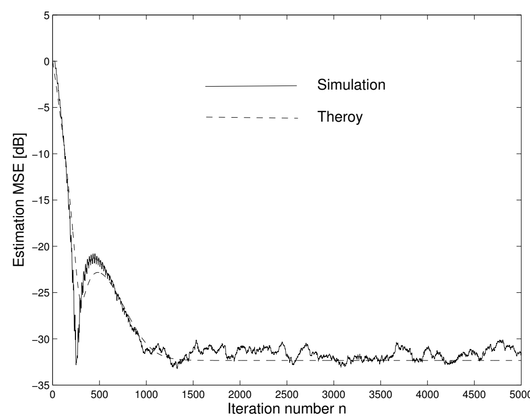

Fig. 4 Comparisons between theory and simulations ($E[\varepsilon^2_{b_1}(n)]$, $M = 41$, $\hat{S}(z) = z^{-22}$ (pure delay), other conditions the same as in Fig.2).

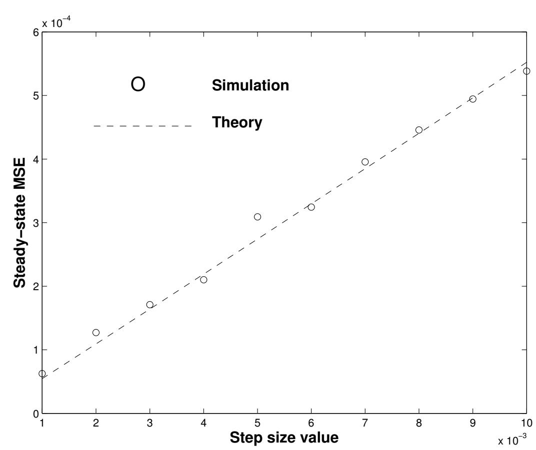

Fig. 5 Comparisons between theory and simulations ($E[\varepsilon^2_{a_1}(\infty)]$, $M = 11$, $\hat{M} = 11$, 40 runs, other conditions the same as in Fig.2).